# 8

# Essential Dynamics on Different Biological Systems: Fis Protein, tvMyb1 Transcriptional Factor and BACE1 Enzyme

Lucas J. Gutiérrez[1,2], Ricardo D. Enriz[1,2] and Héctor A. Baldoni[1,3]
[1]*Área de Química General e Inorgánica*
*Universidad Nacional de San Luis (UNSL), San Luis*
[2]*Instituto Multidisciplinario de Investigaciones Biológicas de San Luis*
*(IMIBIO-SL, CONICET), San Luis*
[3]*Instituto de Matemática Aplicada San Luis (IMASL, CONICET), San Luis*
*Universidad Nacional de San Luis (UNSL)*
*Argentina*

## 1. Introduction

Proteins and enzymes poses a non-covalent 3D structure and therefore their intrinsic flexibility allows the existence of an ensemble of different conformers which are separated by low-energy barriers. These ranges of available conformers for proteins in solution are due to the relative movements among the different domains. Domain motions are important for a variety of protein functions, including catalysis, regulation of activity, transport of metabolites, formation of protein assemblies, and cellular locomotion.

Considering the importance of these conformational changes it is obvious that the different techniques to evaluate these behaviours are very important in order to understand the biological effects. In the present chapter we report molecular dynamics (MD) trajectories analyzed by essential dynamics method on three different molecular systems of biological interest: i) DNA-bending protein Fis (Factor for Inversion Stimulation), ii) DNA-tvMyb1 (*Trichomonas vaginalis* transcriptional factor) and iii) the BACE1 (β–site amyloid cleaving enzyme 1). Although the general structural characteristics for the above systems are well known, comparatively little information is available about their flexibility and dynamics. This is in part due to difficulties with obtaining such information experimentally. Thus, our primary interest was the comparison between the unligated and the complexed state, because the corresponding conclusions may reveal motions of functional relevance.

## 2. Methodology

### 2.1 Molecular dynamics simulations

Twenty-nanoseconds MD simulations were performed for the three systems under study (Fis-protein, DNA- tvMyb1 protein and BACE1 enzyme) in order to relax and investigate the dynamical behaviour of these systems. All the simulations were performed by using the

Amber program (Case et al., 2008). The crystal structure for each system was obtained from the Protein Data Bank (PDB) and such structures were used as the initial model for the different dynamics simulations. The PDB entries were 3IV5, 2KDZ and 1M4H for the DNA-bending protein Fis, DNA-tvMyb1 and BACE1, respectively. An all atom force field was taken from FF99SBilnd (Lindorff-Larsen et al., 2010) for the protein and FF99csc0 (Perez et al., 2007) for the DNA.

Each system was soaked in a truncated octahedral periodic box of TIP3P water molecules. The distance between the edges of the water box and the closest atom of the solutes was at least 10Å. Counterions were added to neutralize the charge of the systems. The entire system was subject to energy minimization in two stages to remove bad contacts between the complex and the solvents molecules. First, the water molecules were minimized by holding the solute fixed with harmonic constraint of strength 100 kcal/molÅ$^2$. Second, conjugate gradient energy minimizations were performed repeatedly four times using positional restraints to all heavy atoms of the receptor with 15, 10, 5 and 0 kcal/molÅ$^2$. The system was then heated from 0 K to 300 K in 300 ps and equilibrated at 300 K for another 200 ps. After the minimization and heating, 20 ns dynamics simulations were performed at the NPT assemble (temperature of 300 K and pressure of 1 atm). During the minimization and MD simulations, particle mesh Ewald (PMD) method was employed to treat the long-range electrostatic interactions in a periodic boundary condition. The SHAKE method was used to constrain hydrogen atoms, allowing a time step for all MD is 2 fs. The direct space non bonded cut-off was of 8Å and initial velocities were assigned from a Maxwellian distribution at the initial temperature.

### 2.2 Essential dynamics

The essential dynamics (ED) method also called Principal Component Analysis (PCA) (Amadei et al., 1993), was used to extract the dimensional subspace in which all biologically relevant motions occur (the so-called essential subspace)( De Groot et al., 1996).

The ED method is based on the diagonalization of the covariance matrix built from atomic fluctuations in a trajectory from which the overall translation and rotations have been removed:

$$C_{ij} = \left\langle \left( X_i - X_{i,0} \right) \left( X_j - X_{j,0} \right) \right\rangle \tag{1}$$

In which X are the separate x, y, and z coordinates of the atoms fluctuating around their average positions $X_0$. $\langle ... \rangle$ represent the average time over the entire trajectory. Here, to construct the protein covariance matrix we have used $C_\alpha$ atom trajectory. Indeed, it has been shown that the $C_\alpha$ atom contains all the information for a reasonable description of the protein large concerted motions (Amadei et al., 1993). Upon the covariance matrix diagonalization a set of eigenvalues and eigenvectors was obtained. The motions along a single eigenvector correspond to concerted fluctuations of atoms. On the other hand, the eigenvalues represent the total mean square fluctuation of the system along the corresponding eigenvectors.

### 2.3 Collective movements

To examine domain motions in a protein we calculated the cross-correlation (normalized covariance) matrix, $C_{ij}$, of the fluctuations of each x, y and z coordinates of the $C_\alpha$ atoms

from their average during the last ten nanosecond of the simulation. The displacement vectors $\Delta r_i$ and $\Delta r_j$ of atoms i and j, the matrix, $C_{ij}$ is given by (Ichiye & Karplus, 1991):

$$C_{ij} = \frac{\left\langle \Delta r_i \times \Delta r_j \right\rangle}{\left( \left\langle \Delta r_i^2 \right\rangle \left\langle \Delta r_j^2 \right\rangle \right)^{1/2}} \tag{2}$$

Where $\Delta r_i$ is the displacement from the mean position of the i-th atom and the angle in brackets represent the average time over the entire trajectory. The elements of the cross-correlation matrix take values from -1 to 1. Positive values of $C_{ij}$ represent a motion in the same direction between atoms i and j, and negative $C_{ij}$ values represent a motion in the opposite direction. When $C_{ij}$ is close to zero, the atomic motions are uncorrelated, and their movements are random compared to each other.

PCA was carried out using the PCAZIP software (Meyer et al., 2006). Geometrical analysis was performed using the ptraj module in AmberTools (Case et al., 2008).

### 2.4 Binding energy decomposition

The MM-GBSA method (Kollman et al., 2000) was applied to the last ten nanosecond of simulation and was used within the one-trajectory approximation. Briefly, the binding affinity for a complex corresponds to the free energy of association written as:

$$\Delta G_{bind} = G_{complex} - \left( G_{receptor} - G_{ligand} \right) \tag{3}$$

In MM-GBSA protocol, the binding affinity in equation (3) is typically calculated using

$$\Delta G = \Delta E_{MM} + \Delta G_{solv} - T\Delta S \tag{4}$$

Where $\Delta E_{MM}$ represents the change in molecular mechanics potential energy upon formation of the complex, calculated using all bonded and non bonded interactions. Solvation free energy penalty, $\Delta G_{solv}$, is composed of the electrostatic component ($G_{GB}$) and a nonpolar component ($G_{NP}$):

$$\Delta G_{solv} = \Delta G_{GB} + \Delta G_{NP} \tag{5}$$

$G_{GB}$ is the polar solvation contribution calculated by solving the GB equation. Dielectric constants of 1 and 80 were used for the interior and exterior, respectively.

The hydrophobic contribution to the solvation free energy, $\Delta G_{NP}$, is estimated using the equation:

$$\Delta G_{NP} = \alpha \ SASA + \beta \tag{6}$$

Where SASA is the solvent-accessible surface area computed by means of the Linear Combination of Pairwise Overlap (LCPO) method (Onufriev et al., 2000) with a solvent probe radius of 1.4 Å. The surface tension proportionality constant $\alpha$ and the free energy of

non polar solvation for a point solute β were set to its standard values, 0.00542 kcal/(mol·Å$^2$) and 0.92 kcal/mol, respectively (Sitkoff et al., 1994).

## 3. Results and discussion

### 3.1 Fis-protein

DNA-binding proteins can broadly be divided into those that recognize their DNA-binding sites with high sequence discrimination and those that bind DNA with little or no obvious sequence preference (Stefano et al., 2010). Examples of the latter class are the nucleoid-associated proteins Fis (Factor for Inversion Stimulation), IHF, UH, and H-NS in eubacteria, chromatin-associated proteins like the HMGB family, and histones in eukaryotes.

Fis protein participates in a wide array of cellular activities such as modulation of DNA topology during growth, (Schneider et al., 1997, 1999) regulation of certain site-specific DNA recombination events, (Betermier et al., 1989; Dorgai et al., 1993; Finkel & Johnson, 1992; Johnson et al., 1986; Kahmann et al., 1985; Weinreich & Reznikoff, 1992) and regulation of the transcription of a large number of genes during different stages of growth, (Kelly et al., 2004; Xu & Johnson, 1995) including ribosomal RNA and tRNA genes and genes involved in virulence and biofilm formation (Bosch et al., 1990; Ross et al., 1990; Falconi et al., 2001; Goldberg et al., 2001; Prosseda et al., 2004; Sheikh et al., 2001; Wilson et al., 2001). In addition, Fis protein can affect various biological processes involved in site-specific DNA recombination, DNA replication, or transcription (Drlica & Rouviere-Yaniv, 1987; Finkel & Johnson, 1992; Schmid, 1990). In some cases, two or more proteins may cooperate in the same process. For example, Fis and HU participate in Hin-mediated DNA recombination (Johnson et al., 1986) and Fis and IHF aid in promoting site-specific recombination of λ DNA (Ball & Johnson, 1991; Johnson et al., 1986; Schneider et al., 1997; Thompson et al., 1987). In other cases, these proteins can play opposing roles, as with Fis and H-NS on transcription of *hns* (Falconi et al., 1996) or IHF and Fis on transcription of *fis* (Pratt et al., 1997).

Regarding the structural aspects, Fis protein is a homodimer composed of two identical 98 amino acid subunits where each Fis subunit contains a β-hairpin (residues 11 to 26) followed by four α-helices (A, B, C, and D) separated by short turns, forming a helix–turn–helix (HTH, residues 74-95) DNA binding motif. Actually it is accepted that Fis protein is joined to non-specific DNA sequences.

The flexion produced by these proteins in the DNA helixes increment the phosphate groups that interacting at the protein flank. The bending of DNA chain is produced because there are two contacts regions between Fis protein and DNA. One is practically fixed during the bending process, while the other slides along the DNA chain. This causes DNA to bend and the twist motions of DNA helix allows the DNA base pair step motions. It appears that there are two different kinds of motions induced by the protein–DNA binding processes. One is the bending or unzipping proceeding along the DNA helical axis, and the other is mainly the base pair opening process which is in the direction orthogonal to the helical axis.

The deviation of the simulated dynamic from the crystal structure was monitored by the temporal evolution of the root-mean-square deviation (RMSD) of $C_\alpha$ atoms. This analysis provides a measure of the structural drift from the initial coordinates as well as the atomic fluctuation over the course of an MD simulation. Most large-scale changes in the overall

RMSD $C_\alpha$ ocurred within 7 ns. From this point, our results indicate that the molecular system is equilibrated and therefore we analysed the last 10 ns of simulation. The value obtained for the RMSD of unligated and complexed forms were 2.40(0.41) and 1.55(0.28) respectively, for the mean value and the standard deviation.

The local protein mobility was analyzed by calculating the average $C_\alpha$ β-factors of unligated and complexed Fis-protein and compared with those values previously reported for the crystal. The β-factors determine the atomic fluctuation in a protein giving information about the flexibility of such structure.

Regarding figure 1a it might be observed that the β-factors obtained for the unligated Fis protein are very similar to those from the experimental data except in determined regions. These regions comprise those amino acids involved in turns, loops and the $\alpha_1$D y $\alpha_2$D helixes.

Figure 1b gives the β-factors analysis for DNA bounded Fis-protein. It can be seen that residues 89-91 and 92-102 show a high mobility because they correspond to the terminal residues of the first subunit and the initial residues of the second one, respectively. With respect to the rest of the regions only small differences are observed and these slight differences might be due to the restricted motion in the crystal.

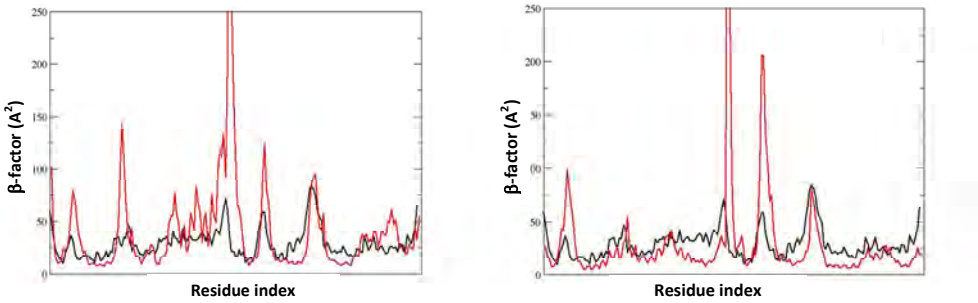


Fig. 1. Thermal factor analysis. MD (red line), experimental (black line).

To analyze the internal motions figure 2 displays the eigenvalues obtained from the diagonalization of the covariance matrix of the atomic fluctuations ranked in a decrement order. The two first eigenvalues represent about 58% and 60% of the collective movement for the unligated and complexed forms, respectively; whereas the last eigenvalues correspond to the small-amplitude vibrations.

In order to evaluate the collective movement, which is determined by the first eigenvector, we projected the last ten ns of the trajectory on the first two eigenvectors. From this resulting trajectory it is possible to calculate a new root-mean-square fluctuation (RMSF) for each residue in order to visualize which residues are the responsible for such movement. Figure 3 shows the RMSF obtained for each residue projected on the first eigenvector for the unligated and complexed forms of Fis protein. The HTH motifs in both subunities displayed a higher mobility at the unligated forms with respect to the complexed form of Fis protein. This is a logical behaviour considering that the HTH motifs are the regions for the binding to DNA. The presences of DNA makes

the HTH motifs much more rigid and increase the mobility in the loops 40-49, 51-64 (subunit 1) and 58-70 (subunit 2) as well as in the helixes $\alpha_2$B.

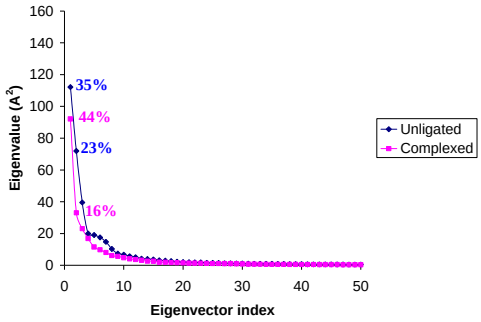


Fig. 2. Comparison between the eigenvalues with the corresponding eigenvector indices obtained from the Ca covariance matrix.

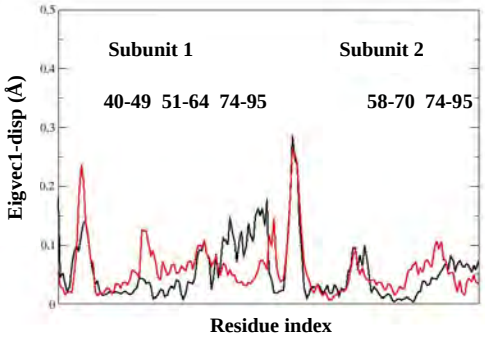


Fig. 3. Residue displacement in the subspace spanned by the first eigenvector. Unligated (black line) and complexed (red line).

Figure 4 gives the movement described the first eigenvector. The red porcupine needles indicate the direction of displacements of motions whereas the size of the needle is proportional to the amount of each displacement. This situation allows us to observe in which direction are moving the previously discussed domains. In short the $\alpha_1$D and $\alpha_2$D domain, which are the mainly responsible of the DNA recognition, are moving in opposite directions (negatively correlated). In addition the $\alpha_1$D domain displayed a higher mobility in comparison to $\alpha_2$D domain. Thus, we can argue that the DNA is gliding by one of the binding regions (HTH motifs whit high mobility), whereas the other binding region is keeping fixed during the flexion process of DNA (HTH with low mobility).

To study the interdomain motions of the residues that make up the dimmer, we examined the correlated maps for the unligated and complexed forms of Fis-protein. Figures 5 a and b display the Dynamics cross-correlation map (DCCM) among the $C_\alpha$ atoms calculated from the MD simulations for the complexed and unligated Fis-protein, respectively. In both cases, unligated and complexed form, the movements are negatively correlated indicating an

expansion and contraction for the binding site located between the HTH motifs of each subunity. On the basis of our results it seems reasonable to argue that this movement is the responsible of DNA flexion.

Figure 6 gives the interaction binding energy decomposition by residue obtained for the complexed Fis protein. In this figure the strength of each interaction might be very well appreciated. Our results are in an almost complete agreement with those reported by Stefano et al. showing that Thr75, Asn73, Gln74, Arg76, Ile83, Asn84, Arg85, Thr87 and Arg89 makes the major contribution for the binding of DNA with Fis protein. It should be noted that only Lys90 is missing in our results in comparison to the experimental data (Stefano et al., 2010).

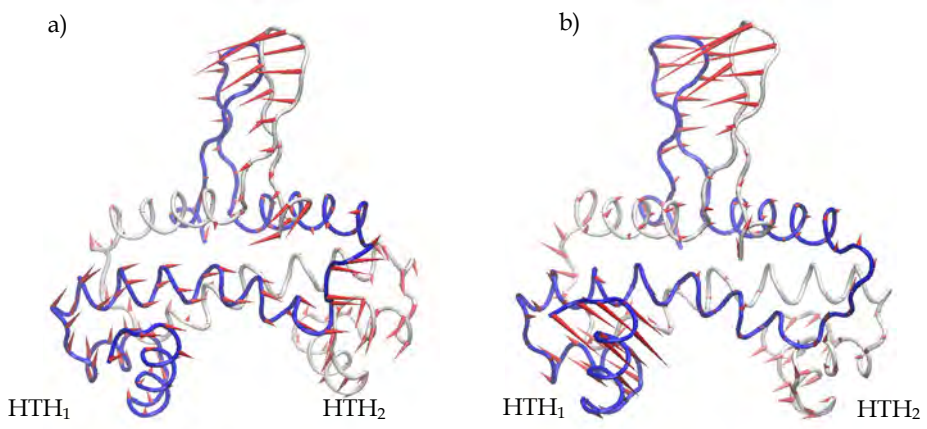


Fig. 4. Porcupine plots obtained for the unligated (a) and complexed (b) forms of Fis protein.

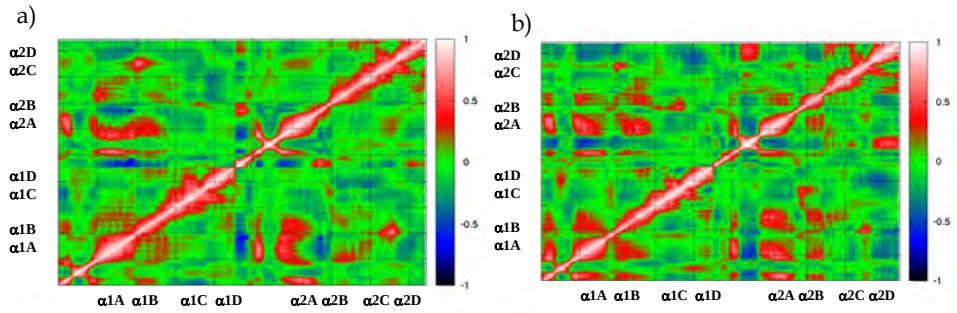


Fig. 5. Cross-correlation matrix obtained for the fluctuations of unligated (a) and complexed (b) forms of Fis protein.

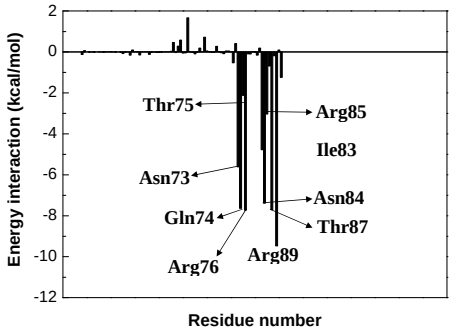


Fig. 6. DNA-Fis protein residue interaction spectrum. The y-axis denotes the interaction energy between the inhibitor and specific residues. The same pattern was observed in both subunities.

### 3.2 tvMyb1 transcriptional factor

The transcription regulator tvMyb1 was the first Myb family protein identified in Trichomonas vaginalis (*T. vaginalis*), a flagellated protozoan parasite of humans, causative agent of trichomoniasis, the most common non-viral sexually transmitted infection worldwide (WHO, 1995). T. vaginalis infection may cause adverse health consequences, including preterm abort and pelvic inflammatory disease in women, as well as infertility and increased incidence of human immunodeficiency virus transmission in women and men (Cotch et al, 1997; Laga et al., 1993; Martinez-Garcia et al., 1996; Moodley et al., 2002; Sherman et al., 1987; Sorvillo et al., 1998).

*T. vaginalis* as other pathogens requires iron for its metabolism. This cation is essential for its growth in the human vagina, where the iron concentration is constantly changing through the menstrual cycle. Iron also favours the adherence of the parasite to vaginal epithelial cells, metabolism and multiplication in culture (Gorrell, 1985; Lehker and Alderete, 1992). In spite of the high prevalence of trichomoniasis and the complications associated with the disease, *T. vaginalis* remains one of the most poorly studied parasites with respect to virulence properties and pathogenesis.

Myb proteins contains DNA-binding domains composed of one, two or three repeated motifs (called R1, R2 and R3 respectively) of approximately 50 amino acids, surrounded by three conserved tryptophan residues (Lipsick, 1996). These tryptophans play a role in the folding of the hydrophobic core of the Myb domains, and are generally conserved in all Myb protein. This hydrophobic core generates the helix-turn-helix (HTH) structure of the DNA-binding domain (Sakura et al., 1989). These HTH motifs recognize the major groove of the target DNA sequences.

Recently, Lou et al. reported the structural basis for the $tvMyb_{35-141}$/DNA interaction investigated using nuclear magnetic resonance, chemical shift perturbations, residual dipolar couplings, and DNA specificity (Lou, 2009). In addition, these authors showed that the $tvMyb_{35-141}$ fragment is the minimal DNA-binding domain encompassing two Myb-like DNA-binding motifs designated as R2 and R3 motifs. Both R2 and R3 motifs consists of three helices adopting a HTH conformations. Both motifs are connected by a long loop. The

published experimental data indicates that the orientation between R2 and R3 motifs dramatically changes upon DNA binding through a number of key contacts involving residues in helices 3 and 6 to the DNA major groove.

A useful method monitoring the flexibility of a protein is the order parameter $S^2$ (Peter et al. 2001; Showalter et al. 2007). This normalized autocorrelation function related to the protein N-H bound vector were evaluated from the equilibrium averaged MD trajectories. $S^2$ gives a measure of the system flexibility, being 1 in a completely rigid system or zero for total flexibility where all the possible conformations are sampled. Figure 7 shows that the calculated $S^2$, during the last ten ns of simulation, for both complexed and unligated forms of the tvMyb1 protein. This figure is in agreement with those obtained from the NMR measurements (Lou et al., 2009). On the basis of such similitude we can argue that the simulated system follows the same trend to that observed from experimental data.

The $S^2$ obtained for the R2 (residues 40-80) domain are 0.74 and 0.79 for the complexed and unligated structures, whereas the $S^2$ obtained for the R3 doma(residues 92-135) in are 0.81 and 0.74 for the complexed and unligated forms, respectively. From these results it might be argue that the R2 of the unligated structure is more rigid than the R2 motif of the complexed form. In turn, the R3 domain of complexed structure is somewhat rigid with respect to the unligated form.

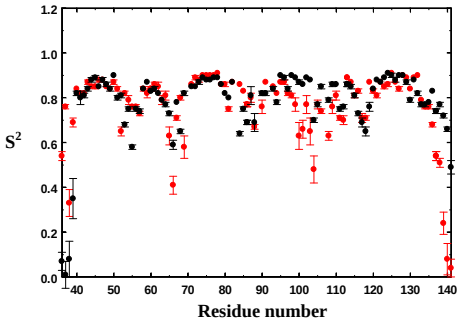


Fig. 7. tvMyb1 backbone N-H bond order parameter profiles from the last 10 ns of trajectory. Complexed form (red circles) and unligated form (black circles).

Figure 8 displays the eigenvalues obtained from the diagonalization of the covariance matrix of the atomic fluctuations ranked in a decrement order. The two first eigenvalues represent about 60% and 65% of the collective movement for the unligated and complexed forms, respectively.

In order to analyse which residues are the responsible of the different movements, we calculate the root-mean-square fluctuation (RMSF) from the equilibrated trajectory. Figure 9a shows the RMSF for each residue projected on the first eigenvector for the unligated and complexed forms of tvMyb1 protein. In this figure it is possible to observe that residues 83-90 on the unligated form show higher fluctuation with respect to that observed for the same residues at the complexed form, the same trend was observed for residues 117-130. In contrast, residues 96-101 display in the complexed form a higher fluctuation than that observed in unligated form.

Figure 9b shows the RMSF for each residue projected on the second eigenvector. In this figure it might be observed that there is not a significant difference in the R2 domain. However residues 79-86 in the unligated form displayed higher flexibility in comparison to the complexed form. On the other hand residue 93-96, 99-104 and 119-121 are more flexible in the complexed form with respect to the unligated form.

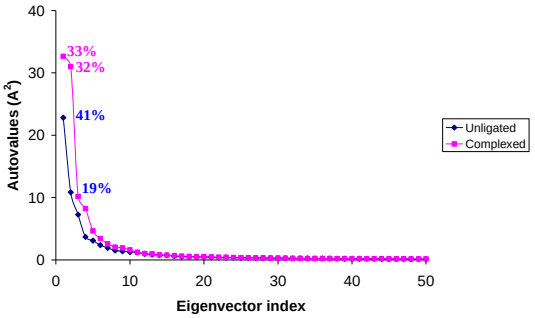


Fig. 8. Eigenvalues plotted against the corresponding eigenvector indices obtained from the Ca covariance matrix.

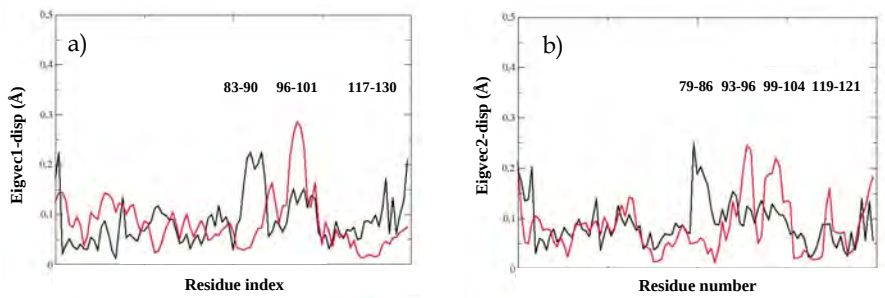


Fig. 9. Residue displacement in the subspace spanned by the first eigenvector (a) and the second eigenvector (b). Unligated and complexed forms are denoted in black and red lines, respectively.

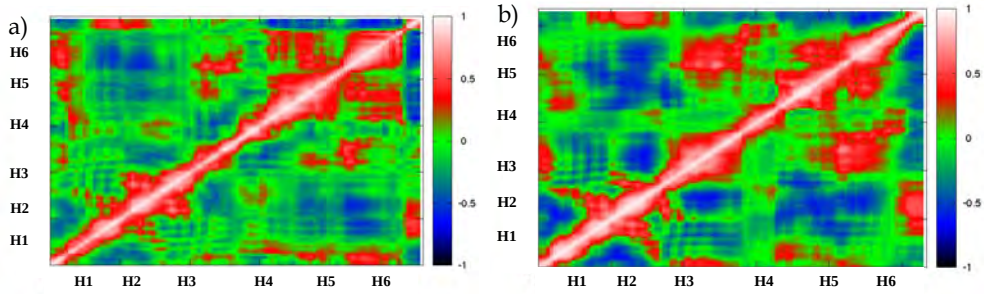


Fig. 10. Cross-correlation matrix obtained for the fluctuations of unligated (a) and complexed (b) forms of tvMyb1 protein.

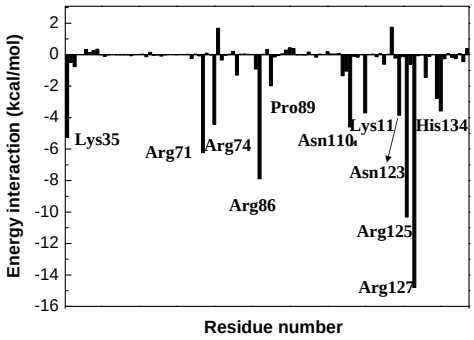


Fig. 11. DNA-tvMyb1 protein residue interaction spectrum. The y-axis denotes the interaction energy between the inhibitor and specific residues.

To better understand the relationship between R2 and R3 domains, we plotted the cross correlation maps for complexed and unligated forms of the tvMyb1 protein (figure 10). Figure 10a gives the cross correlation map obtained for the unligated form. In this figure we can observe that R2 domain (approximately residues 44-72) move in a negatively correlated direction with the R3 domain (approximately residue 97-134). Whereas the H4 and H5 (residues 96-112) move in a positively correlated direction in conjunction with H6 (residues 118-134) in the R3 domain. Figure 10b shows the same behaviour for the complexed form but it should be noted that in this case this movement is somewhat attenuated.

The interaction binding energy decomposition by residue, obtained for the complexed tvMyb1 protein, is show in Figure 11. Our results indicate that residues Lys35, Arg71, Arg74 (R2 domain) , residue Arg86 (loop L1) , and residues Pro89, Asn110, Lys114, Asn123, Arg125, Arg127 and His134 (R3 domain) makes the strongest interactions with the DNA molecule showing that our theoretical results are in agreement with the reported experimental data (Lou, 2009).

### 3.3 BACE1 enzyme

An estimated of 24 million people Worldwide have dementia, the majority of whom are though to have Alzheimer's disease. The two core pathological hallmarks of Alzheimer's disease are amyloid plaques and neurofibrillary tingles. The amyloid cascade hypothesis suggests that deposition of amyloid β (Aβ) triggers neuronal dysfunction and death in the brain.

$A\beta_{42}$ induces neuronal lipid peroxidation and protein oxidation in vivo and in vitro, possibly by generating radicals (Butterfield, 2001, 2003; Hensley et al., 1995) (78–80). Although the neurotoxicity of $A\beta_{42}$ is related to the generation of $H_2O_2$ (Behl et al., 1994) (81) the chemistry involved in generating the oxidation products via $A\beta_{42}$ remains unclear. The Aβ is generated from the amyloid precursor protein (APP) rupture by two proteases: β-site amyloid cleaving enzyme and γ-site amyloid cleaving enzyme (γ-secretase). Thus, β-secretace and γ-secretase are attractive targets for the treatment of AD.

β-secretase, also known as BACE1 (Vassar et al., 1999), memapsin-2 (Lin et al., 2000) and Asp 2 is a membrane-anchored member of the aspartyl protease family of hydrolytic enzymes (Lin et al., 2000). In addition to the active site, some proteolytic enzymes contain additional binding pockets, termed exosites, which engage substrates at locations distal to the active site (Krishnaswamy & Betz, 1997; Maun et al., 2003). These binding pockets on some proteolytic enzymes can act as allosteric regulators of the enzyme activity through conformational changes to the active site, in order to cause an augmentation or diminution of the enzyme's catalytic reactivity (Kornacker et al., 2005). While exosites were reported for serine and cysteine proteases, few examples of exosites have been reported for aspartyl proteases (Kornacker et al., 2005). Recently, we have reported the location for the exosite of BACE1 enzyme (Gutierrez et al., 2010). Considering that this exosite is structurally different to the catalytic site, the features of molecules occupying such exosite could be structurally different to the known mimetic peptides. Thus, molecules possessing the ability to bind to this exosite could be an alternative way to design new and selective inhibitors for the BACE1 enzyme. Here we report how is modified the dynamics behaviour of this enzyme by the presence of an inhibitor in the exosite.

The flexibility of the free BACE1 enzyme has already been reported by Caflisch et al. and by Chakraborty et al. and our simulations are in agreement with these previously reported results. Figures 12a and b gives the experimental and calculated β-factors obtained from the last 10 ns of simulation for free and complexed enzyme, respectively. In both Figures it is possible to appreciate the same general trend. However, in the complexed enzyme the mobility is reduced with respect to free enzyme, due to the presence of the inhibitor.

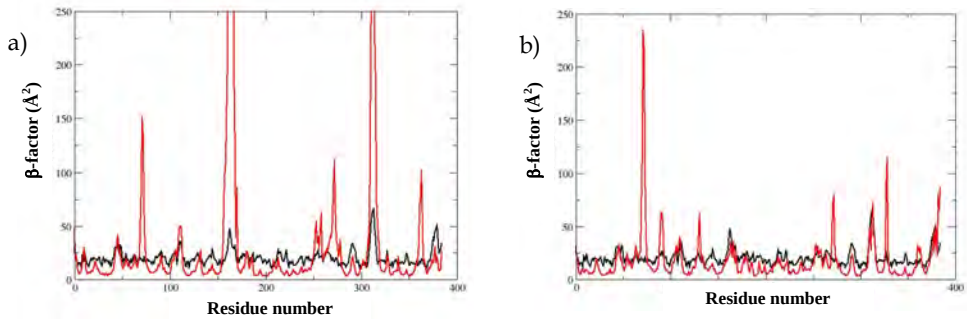


Fig. 12. Thermal factor analysis. MD simulations (red line), experimental data (black line).

In the free and complexed form of BACE1 enzyme it is possible to appreciate different regions with significant mobility. The most representatives are: the 10s loop (residues 9-14), located between two strands at the bottom of the S3 sub pocket; the β-harpin flap (residues 67-77); the A loop (residues 158-167); the F loop (residues 311-318) and D loop (residues 270-273). It is noteworthy to note that the 10s loop, β-harpin flap, A loop loop and F are part of the catalytic cavity.

Figure 13 shows the eigenvalues obtained from the diagonalization of the covariance matrix. Comparing the two models this plot indicates that the presence of the inhibitor in the complexed enzyme decreases the first two eigenvalues drastically with respect to the free form, in accordance with the results shown in Figure 1a) and 1b). The first two eigenvalues

account for approximately 59 and 56% of the collective motion of the complexed and free for of the enzyme, respectively and therefore we focussed our study on these two eigenvectors.

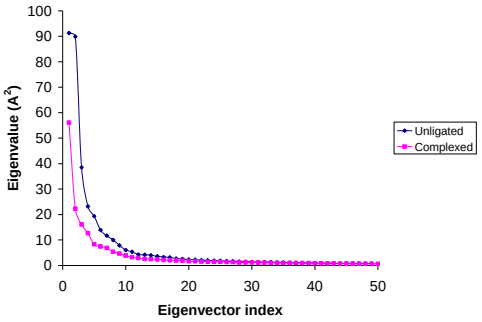


Fig. 13. Eigenvalues plotted against the corresponding eigenvector indices obtained from the Cα covariance matrix.

The motion along any eigenvector can be visualized by projecting all trajectory frames onto a specific eigenvector. Thus, from this new path we calculated the RMSF for the first two eigenvectors (Figure 14). The dynamic behaviour of both forms of the enzyme (i.e. free and complexed) differs in specific areas. In the free form of the enzyme a high mobility was observed for the β-harpin flap and loops A and F, while in the complexed form these regions displayed a similar behaviour. However, loops A and F displayed an attenuated flexibility with respect to the movement on the free enzyme. Another differential behaviour was found in residues 87-93 and 325-330. This behaviour may be relevant because it has been reported that residues 325-330 in the flap are responsible for regulating the ingresses and egress of the BACE1 substrate. (Chakraborty et al., 2011). The collective movement, in for free and complexed form of the enzyme, might be visualized from the porcupine plots in Figures 15 and 16. The collective movement represented by the eigenvectors could be analyzed in two parts a) movement between the N-terminal lobe (residues 1-150) and the C-terminal lobe (residues 151-385), and b) the movement on specific regions that are part of the catalytic cliff.

Figure 14 shows the representation of the first eigenvector for the free and complexed for of the enzyme. Figure 14 a) shows that the C-terminal lobe and N-terminal lobe move in opposite directions. In addition, we see that the β-harpin flap moves toward the catalytic cliff while loops A and F move away, allowing a hinge movement between the lobes. The concerted movements of the above mentioned regions are the ones that dominate the transition between open and closed conformation of BACE1 in agreement with those results reported by Chakraborty. In addition the first eigenvector for the complexed for of the enzyme, Figure 14b displayed an opening between the lobes where the C-terminal lobe moves away from to the N-terminal lobe. It is also possible to appreciate the movement of the β-harpin flap which moves in the opposite direction to the loop 325-330. In the free form of the enzyme, the described movement it is not evident. This finding is very important because these two loops are directly responsible for ingresses and egress of the substrate.

The complexed form of the enzyme (figure 15) displayed a dismissed movement due to the presence of the inhibitor. It is interesting to note that loops A, D and F, which forms part of the exosite, shows a lower movement with respect to the free enzyme due that the inhibitor makes strong interactions with the residues Gln163 (A loop), Trp270 (D loop), Asp311, Thr314 and Asp317 (loop F) in the complexed form of the enzyme as reported by Gutierrez et al. (Gutierrez et al., 2010).

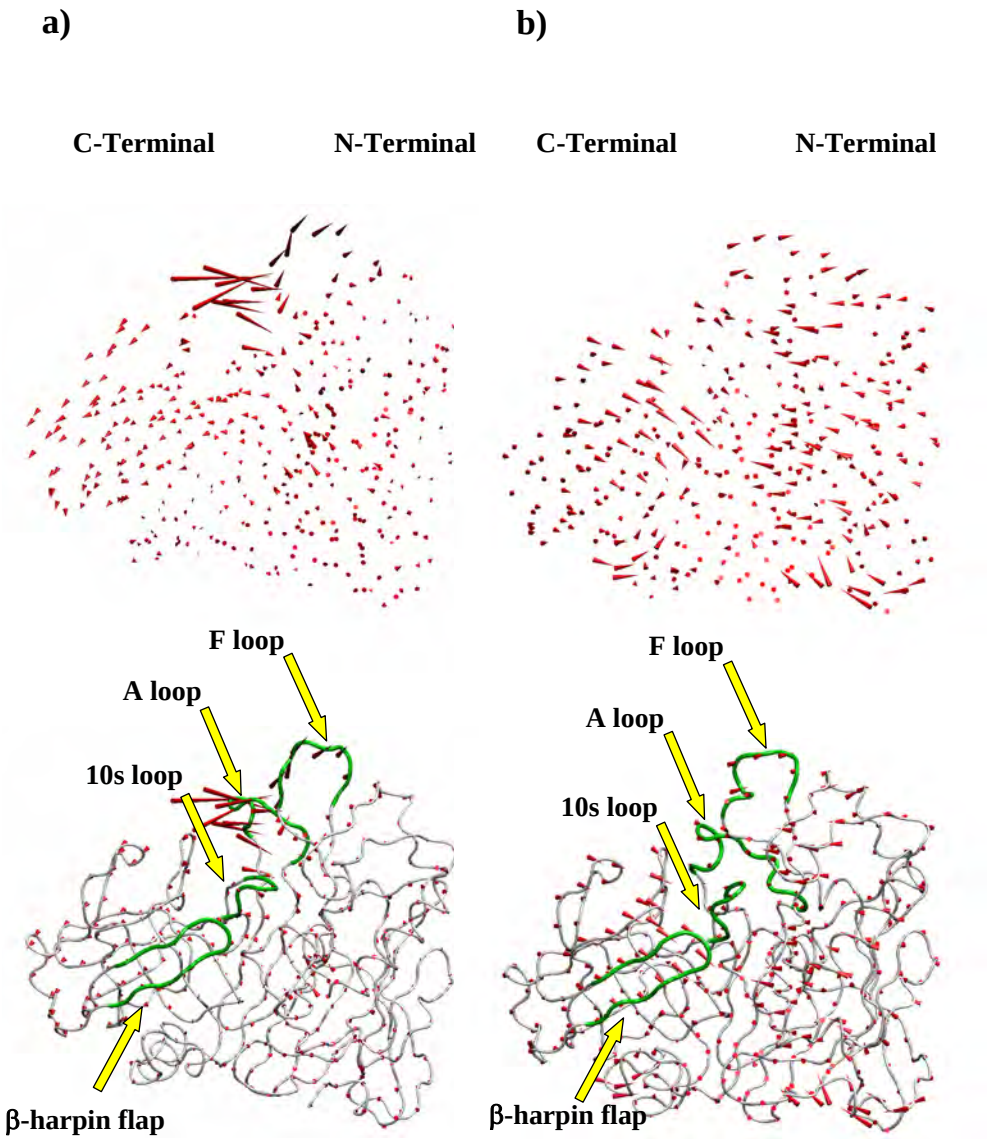


Fig. 14. Porcupine plots obtained for the first a) and second b) eigenvector of the unligated form of BACE1.

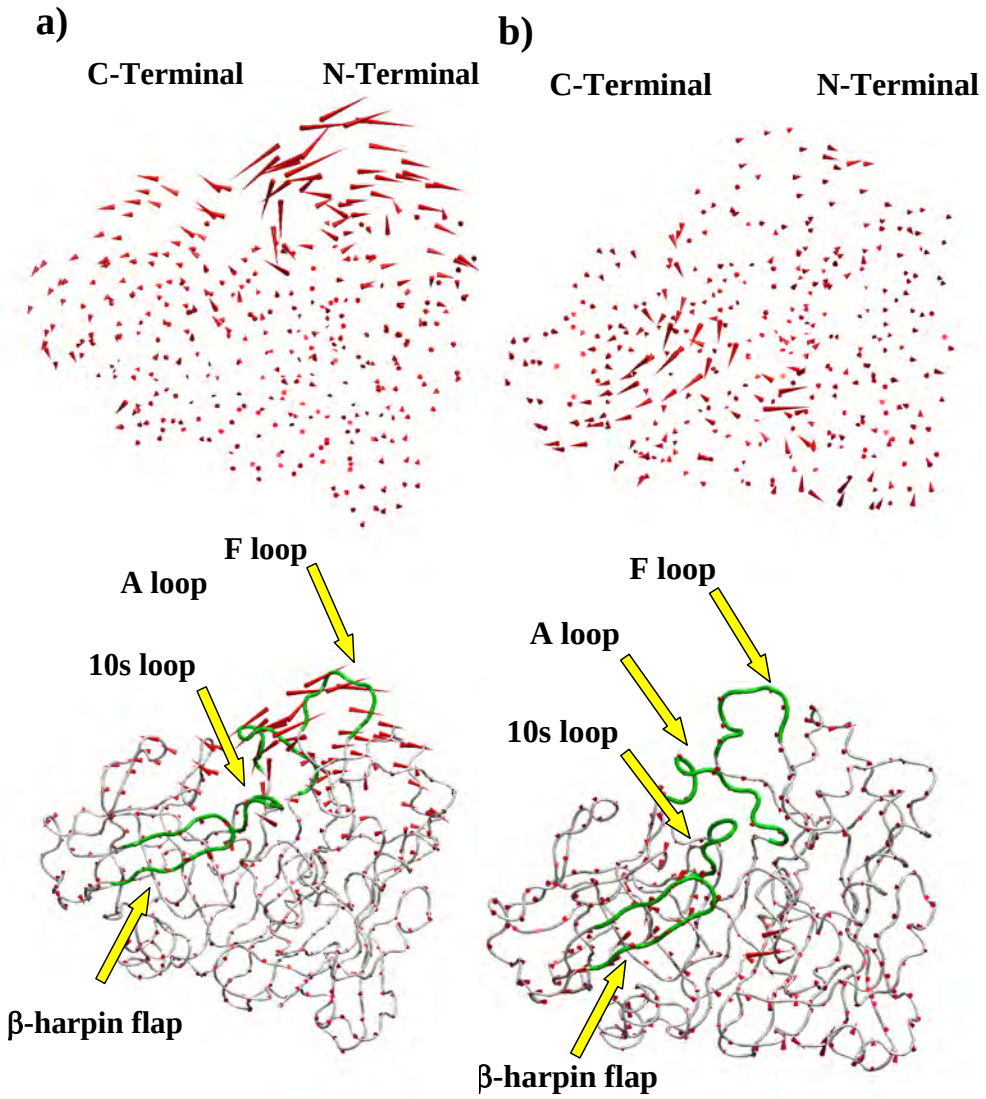


Fig. 15. Porcupine plots obtained for the first a) and second b) eigenvector of the complexed form of BACE1.

## 4. Conclusion

In the present chapter we reported MD simulations performed on three different molecular systems of biological interest: i) DNA-bending protein Fis (Factor for Inversion Stimulation), ii) DNA-tvMyb1 (*Trichomonas vaginalis* transcriptional factor) and iii) the BACE1 (β-site

amyloid cleaving enzyme 1). The model structures proposed accounted for different experimental biological date for these systems indicating that the essential dynamics (ED) method also called Principal Component Analysis (PCA) is a very fruitful tool in order to evaluate the conformational behaviour of molecular systems like reported here. On the other hand, examining the cross-correlation (normalized covariance) matrix, we were able to obtain collective movements which allow examining domain motions for these models. The MM-GBSA methods in turn, allow us to determine binding hot-spots residues as well as the binding energy decomposition giving additional information which in general is very difficult to obtain from experimental data. It is clear that these MD simulations, if it is possible, must be corroborated with accurate experimental data in order to determine their real reaches and limitations. However, it is evident that these theoretical techniques properly applied are very useful and gives additional information to determine the conformational behaviour of complex biological systems.

## 5. Acknowledgments

This work was supported by Universidad Nacional de San Luis (UNSL), Instituto Multidisciplinario de Investigaciones Biológicas de San Luis (IMIBIO-SL, CONICET), Instituto de Matemática Aplicada San Luis (IMASL−CONICET) and Consejo Nacional de Investigaciones Científicas y Técnicas (CONICET−Argentina). L.J.G. gratefully acknowledges a CONICET fellowship; R.D.E. and H.A.B. are staff members of CONICET.

## 6. References

Amadei, A., Linssen, A.B.M., & Berendsen, H.J.C. (1993). Essential dynamics of proteins. *Proteins: Structure, Function and Genetics*, Vol.17, (1993), pp.412-425.

Ball, C. A., & Johnson, R. C. (1991). Efficient excision of phage lambda from the *Escherichia coli* chromosome requires the Fis protein. *Journal of bacteriology*, Vol.173, No. 13, (July 1991), pp.4027–4031.

Ball, C. A., & Johnson, R. C. (1991). Multiple effects of Fis on integration and the control of lysogeny in phage l. *Journal of bacteriology*, Vol.173, No.13, (July 1991), pp.4032–4038.

Behl, C., Davis, J. B., Lesley, R., & Schubert, D. (1994). Hydrogen peroxide mediates amyloid beta protein toxicity. Cell, Vol. 77, No. 6, (June 1994), pp. 817–827

Betermier, M., Lefrere, V., Koch, C., Alazard, R., & Chandler, M. (1989). The Escherichia coli protein, Fis: specific binding to the ends of phage Mu DNA and modulation of phage growth. *Molecular Microbiology*, Vol.3, No. 4, (April 1983), pp.459–468, ISSN 0950-382X

Bosch, L., Nilsson, L., Vijgenboom, E., & Verbeek, H. (1990). FIS-dependent trans-activation of tRNA and rRNA operons of Escherichia coli. *Biochimica et Biophysica Acta*, Vol.1050, No. 1, (August 1990), pp.293–301, ISSN:0006-3002

Butterfield, D. A., Drake, J., Pocernich, C., & Castegna, A. (2001). Evidence of oxidative damage in Alzheimer's disease brain: central role for amyloid β-peptide. *Trends in Molecular Medicine*, Vol.7, No. 12, (December 2001), pp.548–554 ISSN 1471-4914

Butterfield, D. A.: Amyloid β-peptide (1–42)-associated free radical-induced oxidative stress and neurodegeneration in Alzheimer's disease brain: mechanisms and consequences. (2003). *Current Medicinal Chemistry*, Vol. 10, No. 24, (December 2003), pp.2651–2659, ISSN 0929-8673

Case, D.A., Darden, T.A., Cheatham, T.E., Simmerling, C.L., Wang, J., Duke, R.E. Luo, R., Crowley, M., Walker, R.C.W., Zhang Merz, K.M., Wang, B., Hayik, S., Roitberg, A., Seabra, G., Kolossváry, I., Wong, K.F., Paesani, F., Vanicek, J., Wu, X., Brozell, S.R., Steinbrecher, T., Gohlke, H., Yang, L., Tan, C., Mongan, J., Hornak, V., Cui, G., Mathews. D.H., Seetin, M.G., Sagui, C., Babin, V., & Kollman, P.A. AMBER, University of California, San Francisco (2008).

Chakraborty, S., Kumar, S. & Basu, S. (2011). Conformational transition in the substrate binding domain of b-secretase exploited by NMA and its implication in inhibitor recognition: BACE1–myricetin a case study. *Neurochemistry International*, Vol. 58, No. 8, (2011), pp. 914-923, ISSN 0197-0186

Cotch, M. F., Pastorek, J. G., Nugent R. P., Hillier, S. L., Gibbs, R. S., Martin, D. H., Eschenbach, D. A., Edelman, R., Carey, J. C., Regan, J. A., Krohn, M. A., Klebanoff, M. A., Rao, A. V., & Rhoads, G. G. (1997). *Trichomonas vaginalis* associated with low birth weight and preterm delivery: the vaginal infections and prematurity study group. *Journal of the American Sexually Transmitted Diseases*, Vol. 24, No. 6, (July 1997), pp.353-60, ISSN 0148-5717

De Groot, B. L., Van Aalten, D.M.F., Amadei, A., & Berendsen, H.J.C. (1996). The Consistency of Large Concerted Motions in Proteins in Molecular Dynamics Simulations. *Biophysical Journal*, Vol.71, No. 4, (October 1996), pp.1707-1713, ISSN 00063495

Dorgai, L., Oberto, J., & Weisberg, R. A. (1993). Xis and Fis proteins prevent site-specific DNA inversion in lysogens of phage HK022. *Journal of Bacteriology*, Vol.175, No. 3, (Febraury 1993), pp.693–700.

Drlica, K., & Rouviere-Yaniv, J. (1987). Histonelike proteins of bacteria. *Microbiology Reviews,* Vol. 51, No. 3, (September 1987), pp.301–319.

Falconi, M., Brandi, A., Teana, A. L., Gualerzi, C. O., & Pon, C. L. (1996). Antagonistic involvement of FIS and H-NS proteins in the transcriptional control of *hns* expression. *Molecular Microbiology,* Vol.19, No. 5, (March 1996), pp.965–975, ISSN 0950-382X

Falconi, M., Prosseda, G., Giangrossi, M., Beghetto, E., & Colonna, B. (2001). Involvement of FIS in the H-NSmediated regulation of virF gene of Shigella and enteroinvasive Escherichia coli. *Molecular Microbiology,* Vol.42, No.2, (October 2001), pp.439–452, ISSN 0950-382X

Finkel, S. E., & Johnson, R. C. (1992). The Fis protein: it's not just for DNA inversion anymore. *Molecular Microbiology,* Vol.6, No. 22, (1992), pp.3257–3265, ISSN 0950-382X

Goldberg, M. D., Johnson, M., Hinton, J. C., & Williams, P. H. (2001). Role of the nucleoid-associated protein Fis in the regulation of virulence properties of enteropathogenic Escherichia coli. *Molecular Microbiology,* Vol.41, No. 3, (August (2001), pp.549–559, ISSN 0950-382X

Gonzalez-Gil, G., Bringmann, P., & Kahmann, R. (1996). FIS is a regulator of metabolism in Escherichia coli. *Molecular Microbiology*, Vol.22, No. 1, (October 1996), pp.21–29, ISSN 0950-382X

Gorrell, T. E. (1985). Effect of culture medium iron content on the biochemical composition and metabolism of Trichomonas vaginalis. *Journal of Bacteriology*, Vol.161, No. 3, (March 1985), pp.1228–1230.

Gutierrez, L. J., Enriz, R. D., & Baldoni, H. A. (2010). Structural and Thermodynamic Characteristics of the Exosite Binding Pocket on the Human BACE1: A Molecular Modeling Approach. *The Journal of Physical Chemistry A*, Vol. 114, (2010), pp. 10261-10269

Hampel, H., Shen, Y., Walsh, D. M., Aisen, P., Shaw, L. M., Zetterberg, H., Trojanowski, J. Q. & Blennow, K. (2009). Biological markers of amyloid β-related mechanisms in Alzheimer's disease. *Experimental Neurology*, Vol. 223, No. 3, (June 2010), pp.334-346, ISSN 0014-4886

Hensley, K., Hall, N., Subramaniam, R., Cole, P., Harris, M., Aksenov, M., Aksenova, M., Gabbita, S. P., Wu, J. F., Carney, J. M., Lovell, M., Markesbery, W. R., & Butterfield, D. A. (1995). Brain regional correspondence between Alzheimer's disease histopathology and biomarkers of protein oxidation. *Journal Neurochemistry*, Vol. 65, No. 5, (November 1995), pp.2146–2156, ISSN 1471-4159

Ichiye, T., & Karplus, M. (1991). Collective motions in proteins: a covariance analysis of atomic fluctuations in molecular dynamics and normal mode simulations. *Proteins: Structure, Function, and Bioinformatics*, Vol.11, No. 3, (November 1991), pp.205-217, ISSN 1097-0134

Johnson, R. C., Bruist, M. F., & Simon, M. I. (1986). Host protein requirements for *in vitro* site-specific DNA inversion. *Cell*, Vol.46, No.4, (1986) pp.531–539, ISSN 0092-8674

Kahmann, R., Rudt, F., Koch, C., & Mertens, G. (1985). G inversion in bacteriophage Mu DNA is stimulated by a site within the invertase gene and a host factor. *Cell*, Vol41, No. 3, (July 1985), pp.771–780.

Kelly, A., Goldberg, M. D., Carroll, R. K., Danino, V., Hinton, J. C., & Dorman, C. J. (2004). A global role for Fis in the transcriptional control of metabolism and type III secretion in Salmonella enterica serovar Typhimurium. *Microbiology*, Vol.150, No.7, (July 2004), pp.2037–2053.

Kollman, P. A., Massova, I. Reyes, C., Kuhn, B., Huo, S., Chong, L., Lee, M., Lee, T., Duan, Y., Wang, W., Oreola Donini, O., Cieplak, P., Srinivasan, J., Case, D. A. & Cheatham, T. E. (2000). Calculating Structures and Free Energies of Complex Molecules: Combining Molecular Mechanics and Continuum Models. *Accounts of Chemical Research*, Vol. 33, (April 2000), No. 12, pp. 889–897, ISSN 0001-4842

Kornacker, M. G., Copeland, R. A., Hendrick, J., Lai, Z., Mapelli, C., Witmer, M. R., Marcinkeviciene, J., Metzler, W., Lee, V., Riexinger, D. J. (2008). Beta secretase exosite binding peptides and methods for identifying beta secretase modulators. *US Patent 7314726*, Available from: http://www.freepatentsonline.com/7314726.html

Kornacker, M. G., Lai, Z., Witmer, M., Ma, J., Hendrick, J., Lee, V. G., Riexinger, D. J., Mapelli, C., Metzler, W., & Copeland, R. A. (2005). An inhibitor binding pocket distinct from the catalytic active site on human β-APP cleaving enzyme. *Biochemistry*, Vol. 44, No. 34, (August 1997), pp.11567-11573.

Krishnaswamy, S., & Betz, A. (1997). Exosites Determine Macromolecular Substrate Recognition by Prothrombinase. *Biochemistry*, Vol. 36, No. 40, (1997), pp.12080-12086

Laga, M., Manoka, A., Kivuvu, M., Malele, B., Tuliza, M., Nzila, N., Goeman, J., Behets, F., Batter, V., & Alary, M. (1993). Nonulcerative sexually transmitted diseases as risk factors for HIV-1 transmission in women: results from a cohort study. AIDS Vol.7, No. 1, (January 1993), pp.95-102, ISSN 0269-9370

Lehker, M. W., & Alderete, J. F. (1992). Iron regulates growth of Trichomonas vaginalis and the expression of immunogenic trichomonad proteins. *Molecular Microbiology*, Vol.6, No. 1, (January 1992), pp.123–132, ISSN 0950-382X

Lin, X., Koelsch, G., Wu, S., Downs, D., Dashti, A., & Tang, J. (2000). Human aspartic protease memapsin 2 cleaves the beta-secretase site of beta-amyloid precursor protein. *Proceedings of the National Academy of Sciences*, Vol. 97, No. 4, (February 2000), pp. 1456-1460, ISSN 1091-6490

Lindorff-Larsen, K., Piana, S., Palmo, K., Maragakis, P., Klepeis, J.L., Dror, R.O., & Shaw, D.E. (2010). Improved side-chain torsion potentials for the Amber ff99SB protein force field. *Proteins,* Vol.78, No.8, (March 2010), pp.1950-1958, ISSN 08873585

Lipsick, J. S. (1996) One billion years of Myb. *Oncogene*, Vol.13, No. 2, (July 1996), pp.223–235. ISSN 0950-9232

Lou, Y. C., Wei, S. Y., Rajasekaran, M., Chou, C. C., Hsu, H. M., Tai, J. H., & Chen, C. (2009) NMR structural analysis of DNA recognition by a novel Myb1 DNA-binding domain in the protozoan parasite Trichomonas vaginalis. *Nucleic Acids Research*, Vol.37, No. 7, (April 2009), pp.2381-2394.

Martinez-Garcia, F., Regadera, J., Mayer, R., Sanchez, S., & Nistal, M. (1996) Protozoan infections in the male genital tract. *The Journal of Urology*, Vol.156, No. 2, (August 1996), pp.340-349, ISSN 0022-5347

Maun, H. R., Eigenbrot, C., Lazarus RA. (2003). Engineering exosite peptides for complete inhibition of factor VIIa using a protease switch with substrate phage. Journal Biological Chemistry, Vol. 13, No. 24, (March 2003), pp. 21823-21830, ISSN 0021-9258

Meyer, T., Ferrer-Costa, C., Perez, A., Rueda, M., Bidon-Chanal, A., Luque, F. J., Laughton, C. A., & Orozco, M. (2006). Essential dynamics: a tool for efficient trajectory compression and management. *Journal of Chemical Theory and Computation,* Vol.2, No. 2, (February 2006), pp.251–258, ISSN 1549-9618

Moodley, P., Wilkinson, D., Connolly, C., Moodley, J., & Sturm, W. (2002). *Trichomonas vaginalis* is associated with pelvic inflammatory disease in women infected with HIV. *Clinical Infectious Diseases*, Vol.34, No. 4, (2002), pp.519-522.

Onufriev, A., Bashford, D., & Case, D. A. (2000). Modification of the generalized Born model suitable for macromolecules. *The Journal of Physical Chemistry B*, Vol. 104, No. 15, (March 2000), pp. 3712–3720.

Pérez, A., Marchán, I., Svozil, D. Sponer, J., Cheatham, T. E., Laughton, C. A. & Orozco, M. (2007). Refinement of the AMBER Force Field for Nucleic Acids: Improving the Description of □/□ Conformers. *Biophysical Journal*, Vol. 92., No. 11, (June 2007), pp. 3817-3829, ISSN 00063495

Peter, C., Daura, X., & van Gunsteren, W. F. (2001). Calculation of NMR-relaxation parameters for flexible molecules from molecular dynamics simulations. Journal of Biomolecular NMR, Vol.20, No. 4, (May 2001), pp.297–310.

Pratt, T. S., Steiner, T., Feldman, L. S., Walker, K. A., & Osuna, R. (1997). Deletion analysis of the *fis* promoter region in *Escherichia coli*: antagonistic effects of integration host factor and Fis. *J. Bacteriol.*, Vol.179, No. 20, (October 1997), pp.6367–6377.

Prosseda, G., Falconi, M., Giangrossi, M., Gualerzi, C. O., Micheli, G., Colonna, B. (2004). The virF promoter in Shigella: more than just a curved DNA stretch. *Molecular Microbiology*, Vol.51, No. 2, (January 2004), pp.523–537, ISSN 0950-382X

Ross, W., Thompson, J. F., Newlands, J. T., & Gourse, R. L. (1990). E. coli Fis protein activates ribosomal RNA transcription in vitro and in vivo. *EMBO Journal*, Vol.9, No. 11, (November 1990), pp.3733–3742.

Sakura, H., Kanei-Ishii, C., Nagase, T., Nakagoshi, H., Gonda, T. J., & Ishii, S. (1989). *Proc. Natl. Acad. Sci*., Vol.86, pp.5758–5762.

Schmid, M. B. (1990). More than just "histone-like" proteins. *Cell* Vol.63, No. 3, (November 1990), pp.451–453.

Schneider, R., Travers, & A., Muskhelisvili, G. (1997). FIS modulates growth phase-dependent topological transitions of DNA in *Escherichia coli*. *Molecular Microbiology*, Vol.26, No.3, (1997), pp.519–530, ISSN 0950-382X

Schneider, R., Travers, A., & Muskhelishvili, G. (1997). Fis modulates growth phase-dependent topological transitions of DNA in Escherichia coli. *Molecular Microbiology,* Vol.26, No. 3, (October 1997), pp.519–530, ISSN 0950-382X

Schneider, R., Travers, A., Kutateladze, T., & Muskhelishvili, G. (1999). ADNA architectural protein copules cellular physiology and DNA topology in Escherichia coli. *Molecular Microbiology*, Vol.34, No. 5, (December 1999), pp.953–964, ISSN 0950-382X

Sheikh, J., Hicks, S., Dall'Agnol, M., Phillips, A. D., & Nataro, J. P. (2001). Roles for Fis and YafK in biofilm formation by enteroaggregative Escherichia coli. *Molecular Microbiology,* Vol.41, No. 5, (September 2001), pp.983–997, ISSN 0950-382X

Sherman, K. J., Daling, J. R., & Weiss, N. A. (1987). Sexually transmitted diseases and tubal infertility. *Journal of the American Sexually Transmitted Diseases*, Vol.14, No. 1, (1987), pp.12-6, ISSN 0148-5717

Showalter, S.A., & Brüschweiler, R. (2007). Validation of molecular dynamics simulations of biomolecules using NMR spin relaxation as benchmarks: Application to the AMBER99SB force field. Journal of Chemical Theory and Computation. Vol. 3, No 3, (January 2007). pp. 961-975.

Sitkoff, D., Sharp, K., & Honing, B. *J.* (1994). *The Journal of Physical Chemistry,* Vol. 98, No. 7, (February 1994), pp.1978–1988.

Sorvillo F., & Kerndt P. (1998). *Trichomonas vaginalis* and amplification of HIV-1 transmission. *The Lancet,* Vol.351, No. 9097, (January 1998), pp.213-4. ISSN 0140-6736

Stella, S., Cascio, D., & Johnson R. C. (2010). The shape of the Dna minor groove directs binding by the DNA-bending protein Fis. *Genes & Development*, Vol. 24, (August 2010), pp.814-826, ISSN 0890-9369/10.

Thompson, J. F., Moitoso de Vargas, L., Koch, C., Kahmann, R., & Landy, A. (1987). Cellular factors couple recombination with growth phase: characterization of a new component in the lambda site-specific recombination pathway. *Cell*, Vol.50, No. 11, (September 1987), pp.901–908.

Vassar, R., Bennett, B. D., Babu-Khan, S., Kahn, S., Mendiaz, E. A., Denis, P., Teplow, D. B., Ross, S., Amarante, P., Loeloff, R., Luo, Y., Fisher, S., Fuller, J., Edenson, S., Lile, J., Jarosinski, M. A., Biere, A. L., Curran, E., Burgess, T., Louis, J. C., Collins, F., Treanor, J., Rogers, G. & Citron, M. (1999). β-Secretase Cleavage of Alzheimer's Amyloid Precursor Protein by the Transmembrane Aspartic Protease BACE. *Science,* Vol. 286, No. 5440, (October 1999), pp. 735-741, ISSN 0036-8075

Weinreich, M. D., & Reznikoff, W. S. (1992). Fis plays a role in Tn5 and IS50 transposition. *Journal of Bacteriology*, Vol.174, No. 14, (July 1992), pp.4530–4537.

Wilson, R. L., Libby, S. J., Freet, A. M., Boddicker, J. D., Fahlen, T. F., & Jones, B. D. (2001). Fis, a DNA nucleoid-associated protein, is involved in Salmonella typhimurium SPI-1 invasion gene expression. *Molecular Microbiology*, Vol.39, No. 1, (February 2001), pp.79–88, ISSN 0950-382X

World Health Organization. 1995. An Overview of Selected Curable Sexually Transmitted Disease. In: World Health Organization (ed), Global program of AIDS. Geneva, Switzerland, pp. 2–27.

Xu, J., & Johnson, R. C. (1995). Identification of genes negatively regulated by Fis: Fis and RpoS comodulate growth-phase-dependent gene expression in Escherichia coli. *Journal of Bacteriology*, Vol.177, No. 4, (February 1995), pp.938–947.